Journal of
Water & Climate Change

IWA PUBLISHING

Journal of Water and Climate Change Vol 14 No 8, 2564 doi: 10.2166/wcc.2023.447

Projected changes in extreme precipitation indices over the Lake Urmia basin in Iran

Khadijeh Javan [a,b], Alireza Movaghari [a,b] and Jeong-Soo Park [c,*]

[a] Department of Geography, Urmia University, Urmia, Iran
[b] Urmia Lake Research Institute, Urmia University, Urmia, Iran
[c] Department of Statistics, Chonnam National University, Gwangju, Korea
*Corresponding author. E-mail: jspark@jnu.ac.kr

KJ, 0000-0002-1005-5051; J-SP, 0000-0002-8460-4869

ABSTRACT

This study investigates the future changes in precipitation extreme indices in the Lake Urmia Basin during the period 2021–2100 compared to the base period (1987–2016), using the Coupled Model Intercomparison Project Phase 5 models. Trend analysis was performed using Mann–Kendall test and Sen's estimator. The output of these models was downscaled by the Long Ashton Research Station Weather Generator method for the representative concentration pathway (RCPs) 4.5 and 8.5. A model averaging technique was employed to create an ensemble model. The results showed that the average precipitation of the basin will decrease by the end of the 21st century. The projection also showed that the consecutive dry day's index increases based on both scenarios. However, other indices (maximum 1-day precipitation, maximum 5-day precipitation, very wet days, consecutive wet days, simple daily intensity index, and wet-day precipitation) are reduced compared to the base period. Moreover, the slope of significant trends in the RCP8.5 is greater and more severe than that in RCP4.5.

Key words: ensemble, GCMs, precipitation extremes, statistical downscaling, water resources

HIGHLIGHTS

- This study focuses on the future change of extreme rainfall in the Lake Urmia basin in Iran.
- The projected results are decreasing trends in extreme precipitation and in wet days and increasing trends in dry days by the end of the 21st century.
- This study predicts that the basin may face more drought in the future.
- The results of this study have important implications for the management of water resources.

GRAPHICAL ABSTRACT

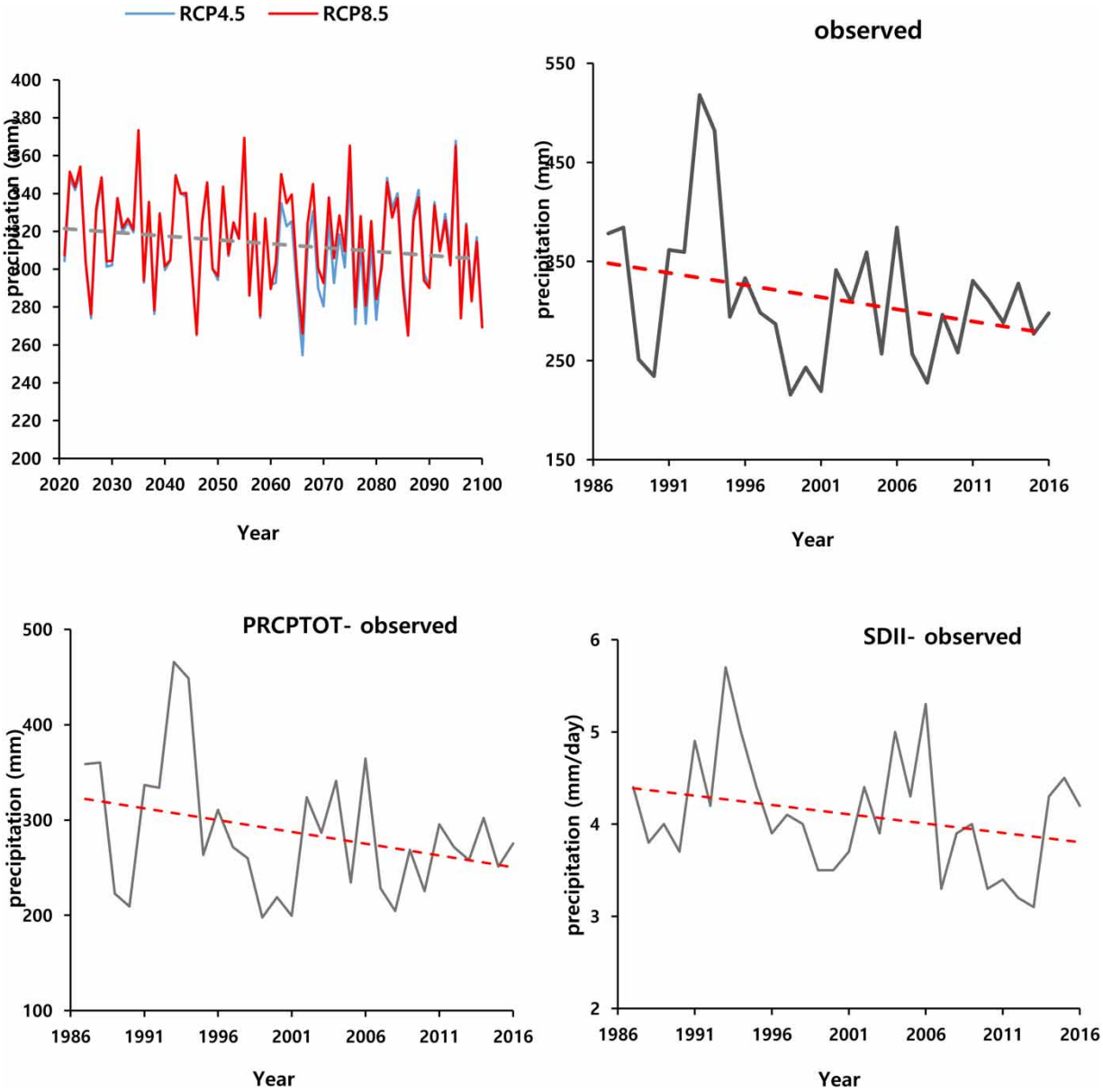

1. INTRODUCTION

Climate change is already affecting global ecosystems, biodiversity, social economics, and human health (IPCC 2013; Ashktorab & Zibaei 2022; Esa *et al.* 2022). Therefore, it is important for scientists to assess the effects of climate change in each region and provide proper solutions to adapt and reduce the consequences of climate change (Fuhrer 2003). The Intergovernmental Panel on Climate Change (IPCC) in the Fifth Assessment Report (AR5) reported that climate warming is quite clear, and the continued greenhouse gas emissions cause more warming and change in all parts of the climate system (IPCC 2013). One of the important consequences of climate change will be the increase in extreme climate phenomena such as droughts, floods, hail, heat waves, rising sea levels, and cold waves (Hu *et al.* 2012). The previous study indicates that the intensity and the frequency of extreme precipitation events in the mid-latitudes may further increase in the future (IPCC 2013). Any change in the intensity or frequency of climatic extremes can have great effects on the natural environment and human societies. Therefore, analyzing extreme events is very important.

In this regard, a set of climate extreme can be used for the analysis of extreme precipitation amounts (e.g., Sillmann *et al.* 2013; Xu *et al.* 2018; Lee *et al.* 2020; Grover *et al.* 2022; Hong *et al.* 2022). Some researchers have conducted various studies on changes in climate extremes for both observational and future periods. On the other hand, many studies have focused mainly on assessing changes and trends in mean observational climate values in the last decades. On the basis of studies on observed data, Rahimzadeh *et al.* (2009), Soltani *et al.* (2016), Azizzadeh & Javan (2018), and Fathian *et al.* (2020) showed that the extreme precipitation indices in some regions of Iran, such as dry and wet days, have increased and decreased, respectively.

Climate change forecasts rely on general circulation models (GCMs). The GCMs, as numerical models representing the physical processes of the atmosphere, can simulate the current climate and visualize future climate situations based on various scenarios (Sillmann *et al.* 2013; Lee *et al.* 2020; Abbasi *et al.* 2022). As a collection of GCMs, CMIP5 (Coupled Model Intercomparison Project Phase 5) models have higher horizontal resolutions than previous CMIPs and also have much more comprehensive behavior in relation to physical processes such as vegetation feedbacks, aerosols, and land cover types (Aloysius *et al.* 2016). Unlike the Special Report on Emissions Scenarios (SRES), in the representative concentration pathway (RCP) scenarios, the forcing radiation path is not predefined, and the RCPs are able to represent different combinations of economic status, demographics technology, and political development (Moss *et al.* 2010). It is, therefore, expected that the errors of the CMIP5 models will be reduced compared to the previous models and also provide more realistic simulations of the future (Taylor *et al.* 2012).

Because the outputs of GCMs are large-scale gridded, there is a discrepancy between the scale of these models and the scale needed to study the effects of climate change. This has led to the development of several downscaling methods (Graham *et al.* 2007). LARS-WG (Long Ashton Research Station Weather Generator), which is employed in this study, is one of the statistical models that many evaluations have been made with this model and acceptable results have been obtained (Reddy *et al.* 2014; Kavwenje *et al.* 2022).

In Iran, Zamani Noori *et al.* (2014) investigated the uncertainty of precipitation and temperature parameters simulated by two downscaling models, namely, LARS-WG and statistical downscaling model (SDSM). The results showed that the LARS-WG performs better than the SDSM in precipitation simulation and shows a decrease in precipitation in the near future. Goudarzi *et al.* (2015) in simulating climate change in the Lake Urmia basin with LARS-WG and SDSM showed that the SDSM model is more successful in simulating temperature parameters and has less uncertainty, while the LARS-WG model is better in simulating rainfall periods. Lotfi *et al.* (2022) analyzed the performance of LARS-WG and SDSM in simulating temperature and precipitation changes in the West of Iran. They showed that LARS-WG is more efficient in simulating annual precipitation and is simpler with a higher performance speed. Zarrin *et al.* (2022) evaluated future changes in some precipitation extremes over Iran for the historical and future periods based on five CMIP6 bias-corrected models.

Lake Urmia, the largest inland lake in Iran, plays a great role in moderating the climate of the region. In the basin of this lake, agricultural and industrial activities, as well as infrastructure projects and water resources development, have expanded in recent decades (Taheri *et al.* 2019). These actions have had important effects on the ecological conditions and level of Lake Urmia. Climate change, on the other hand, plays an important role in Urmia Lake's water level and water resources (Abbaspour *et al.* 2012). Research has shown that water resources have declined in watersheds such as Lake Urmia (Delju *et al.* 2013). Therefore, it is necessary to examine climate change, especially in the Lake Urmia basin, which has become an environmental crisis (AghaKouchak *et al.* 2015). Attention to the new scenarios and models is also necessary to better understand the behavior of climate change in the basin in the future.

The purpose of this study is to investigate the change of extreme precipitations in the Lake Urmia basin using the output of CMIP5 models and RCP in the base period (1987–2016) and the future periods (2021–2100). This study attempts to:

- select the most suitable model for the basin from the CMIP5 models and to construct an ensemble model to reduce uncertainty,
- downscale the precipitation during the reference period, and
- provide a prospect of changes in extreme indices over the studied periods.

Considering the critical situation of the water resources of the Lake Urmia basin, we believe that this study is very necessary for the sustainable exploitation of the basin's water resources under climate change.

2. MATERIALS AND METHODS

2.1. Study area

Lake Urmia is approximately 5,750 km^2 in the middle of the northern part of the basin. This lake has been registered as a protected environmental heritage by the United Nations because of its unique ecological environment (Soudi *et al.* 2017). Lake Urmia is the 20th largest and the second Supersaturated Salt Lake in the world. The Lake Urmia Basin with an area of about 51,800 km^2 is located between 35° 10′ to 38° 30′ N and 44° 14′ to 47° 53′ E in northwestern Iran (Figure 1). Precipitation changes in the Lake Urmia Basin are 220–450 mm, and the average rainfall is 310 mm. The rainfall increased from the central part of the basin to the peripheral highlands. In this basin, the average rainfall decreased by about 9.2%, and the mean maximum temperature has increased to about 0.8 °C (Delju *et al.* 2013).

One of the main problems is the decrease in the water level of Lake Urmia in recent years, which seems to have affected the climate change in addition to the construction of numerous dams and the expansion of gardens and agriculture (Khazaei *et al.* 2019). At present, the lake's water level has decreased more than 6 m from the peak and nearly 3 m from the ecological level (Tourian *et al.* 2015). So far, research studies have been conducted on the future status of rainfall and runoff in the Lake Urmia basin using different models (Goudarzi *et al.* 2015; Davarpanah *et al.* 2021). But there has been no research on the impacts of climate change on extreme precipitation indices in this basin, as far as the authors know.

2.2. Data collection and quality assessment

The data used in this research include daily precipitation data, minimum temperature, maximum temperature, and number of sunshine hours at eight synoptic stations in the basin that have long-term and reliable data. These data are for the period 1987–2016. Missing data for each station were replaced with daily averages from other years obtained from the same station (Liu *et al.* 2011). The distribution of the synoptic stations is shown in Figure 1, and the characteristics of these stations are provided in Table 1. In the first step, data quality control and homogeneity were investigated using the RClimDex package.

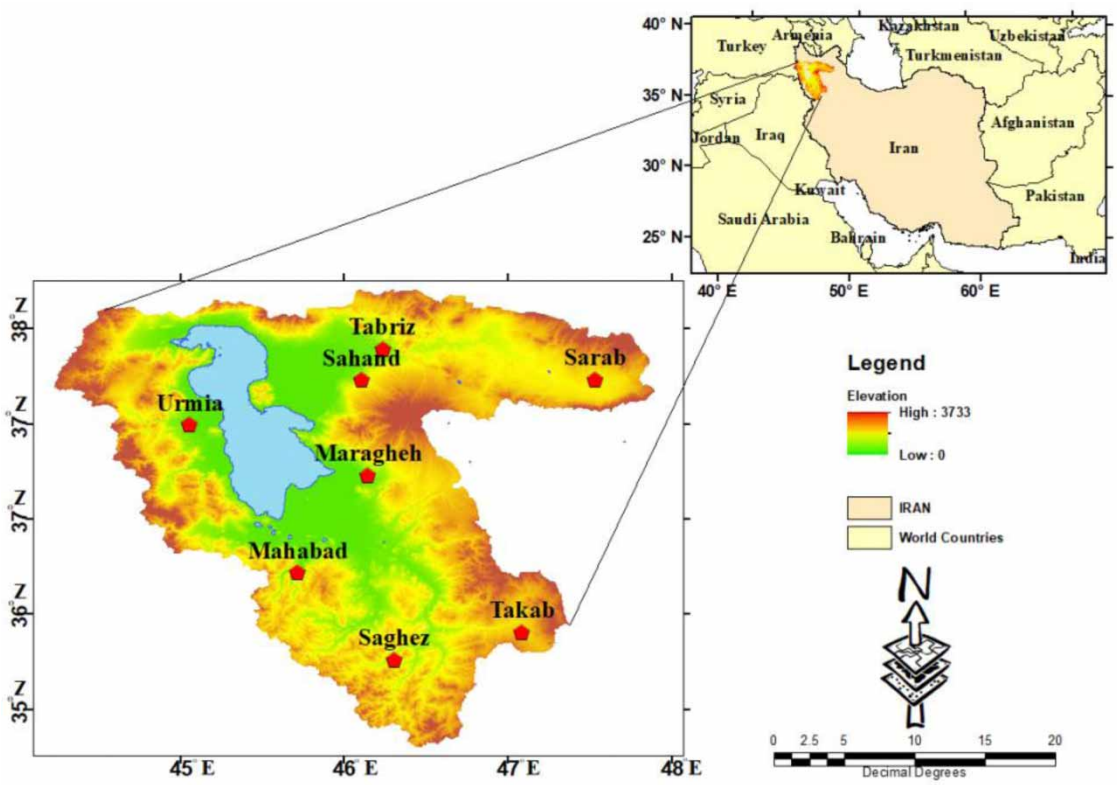

Figure 1 | Geographical location of the Lake Urmia Basin.

Table 1 | List of stations with altitude, latitude, and longitude in the Lake Urmia Basin

Station	Altitude (m)	Latitude (N)	Longitude (E)
Mahabad	1,500	36° 46′	45° 43′
Maragheh	1,477.7	37° 24′	46° 16′
Urmia	1,316	37° 32′	45° 05′
Saghez	1,552.8	36° 14′	46° 16′
Sahand	1,641	37° 56′	46° 07′
Sarab	1,682	37° 56′	47° 32′
Tabriz	1,361	38° 05′	46° 17′
Takab	1,765	36° 23′	47° 7′

2.3. Future climate data

Future period data are based on the output of CMIP5 models. Despite the development of climate models and the advancement of science, there are some biases and uncertainty in models (IPCC 2013). Various methods have been proposed by IPCC to reduce these uncertainties. One of these methods is to identify suitable GCMs that reduce uncertainty in future simulations. Table 2 presents the details of 16 models from the CMIP5, which were used for this study.

For validation of models, we employed the following performance measures: coefficient of determination (R^2), mean absolute error (MAE), root mean square error (RMSE), mean bias error (MBE), and mean percentage error (MPE). For this purpose, two datasets including observed precipitation of basin synoptic stations and output of 16 CMIP5 models for the period (1987–2016) were examined. The equations of these statistical measures are provided in Equations (1)–(5).

$$R^2 = \frac{\sum_{i=1}^{N}(S_i - \bar{S})(O_i - \bar{O})}{\sqrt{\sum_{i=1}^{N}(S_i - \bar{S})(O_i - \bar{O})^2}} \quad (1)$$

Table 2 | Description of global climate models from the CMIP5 ensemble used in this study

Model	Country	Grid resolution
BCC-CSM1.1	China	2.77° × 2.81°
CanESM2	Canada	2.77° × 2.81°
CNRM-CM5	France	1.40° × 1.40°
CSIRO-MK36	Australia	1.85° × 1.88°
EC-EARTH	Europe	1.125° × 1.125°
GFDL-CM3	USA	2.00° × 2.50°
GISS-E2-R-CC	USA	2.00° × 2.50°
HadGEM2-ES	UK	1.25° × 1.88°
IPSL-CM5A-MR	France	1.27° × 2.50°
MIROC5	Japan	1.39° × 1.41°
MIROC-ESM	Japan	2.77° × 2.81°
MPI-ESM-MR	Germany	1.85° × 1.88°
MRI-CGCM3	Japan	1.11° × 1.13°
NCAR-CCSM4	USA	0.94° × 1.25°
NCAR-CESM1-CAM5	USA	0.94° × 1.25°
NorESM1-M	Norway	1.90° × 2.50°

$$\text{MAE} = \frac{\sum_{i=1}^{N} |S_i - O_i|}{N} \tag{2}$$

$$\text{RMSE} = \sqrt{\frac{1}{N}\sum_{i=1}^{N} (S_i - O_i)^2} \tag{3}$$

$$\text{MBE} = \frac{\sum_{i=1}^{N} (S_i - O_i)}{N} \tag{4}$$

$$\text{MPE} = \frac{\sum_{i=1}^{N} \left(\frac{|O_i - P_i|}{O_i}\right) \times 100}{N} \tag{5}$$

where S_i is the precipitation estimated from the model, O_i is the observed precipitation, and N is the total number of observations.

Considering the complexity of the climate system, it is hard to adequately describe climate change with a single model. To reduce uncertainty, the average or a combination of results from several models has been used for climate projections. Model averaging is a statistical method in which unequal or equal weights are assigned to those models (Hong *et al.* 2021). In this study, equally weighted model averaging was used to ensemble the selected models.

Because the output of GCMs does not have the necessary capability at the local scale, downscaling methods should be used to compensate for this shortcoming. In this regard, the LARS-WG downscaling method was used based on the scenarios of RCP4.5 and RCP8.5. The RCP4.5 represents the intermediate scenario, while the RCP8.5 is the most pessimistic scenario (Moss *et al.* 2010). In RCP4.5 (RCP8.5), the CO_2 concentration by the year 2100 is 650 ppm (1,370 ppm), and the effect of greenhouse gases on radiative forcing is 4.5 W/m^2 (8.5 W/m^2) (Van Vuuren *et al.* 2011).

LARS-WG is one of the popular methods for generating stochastic weather data and has been used to produce minimum and maximum temperatures, precipitation, and radiation on a daily basis under present and future climatic conditions (Kilsby *et al.* 2007). This method has a high ability to predict the climate change (Semenov & Stratonovitch 2010). To implement the LARS-WG in this study, daily maximum and minimum temperature, sunshine hours, and precipitation data over a 30-year period (1987–2016) were used. The general methodology diagram is shown in Figure 2.

2.4. Extreme precipitation indices

Eight extreme precipitation indices introduced by ETCCDMI (Expert Team on Climate Change Detection, Monitoring and Indices) were used in this study. The list of these indices is presented in Table 3. All of these indices are estimated by RClimDex (Zhang & Yang 2004). These indicators can be grouped into four classes (Alexander *et al.* 2006):

1. *Percentage indices:* Precipitation over the 95th percentile (R95p) and 99th percentile (R99p), and 1-year extreme precipitation events.
2. *Absolute indices:* Maximum 1-day precipitation (RX1day) and maximum 5-day precipitation (RX5day).
3. *Periodic indices:* Consecutive wet days (CWDs), and consecutive dry days (CDDs).
4. *Other indices:* Simple daily intensity index (SDII), and the annual wet day precipitation (PRCPTOT).

2.5. Trend detection

The Mann–Kendall (MK) test was used to examine the trend in the long-term observation series. In this test, H_0 indicates the absence of a trend and H_1 indicates the trend in the data. Let $X_1, X_2, \ldots, X_n$ be a series of n observations, where X_j represents an observation at time j. Then, the MK test (S) is expressed by Equations (6)–(9) (Tabari & Talaee 2011; Wilks 2011):

$$S = \sum_{i=1}^{n-1} \sum_{j=i+1}^{n} \text{sgn}(x_j - x_i) \tag{6}$$

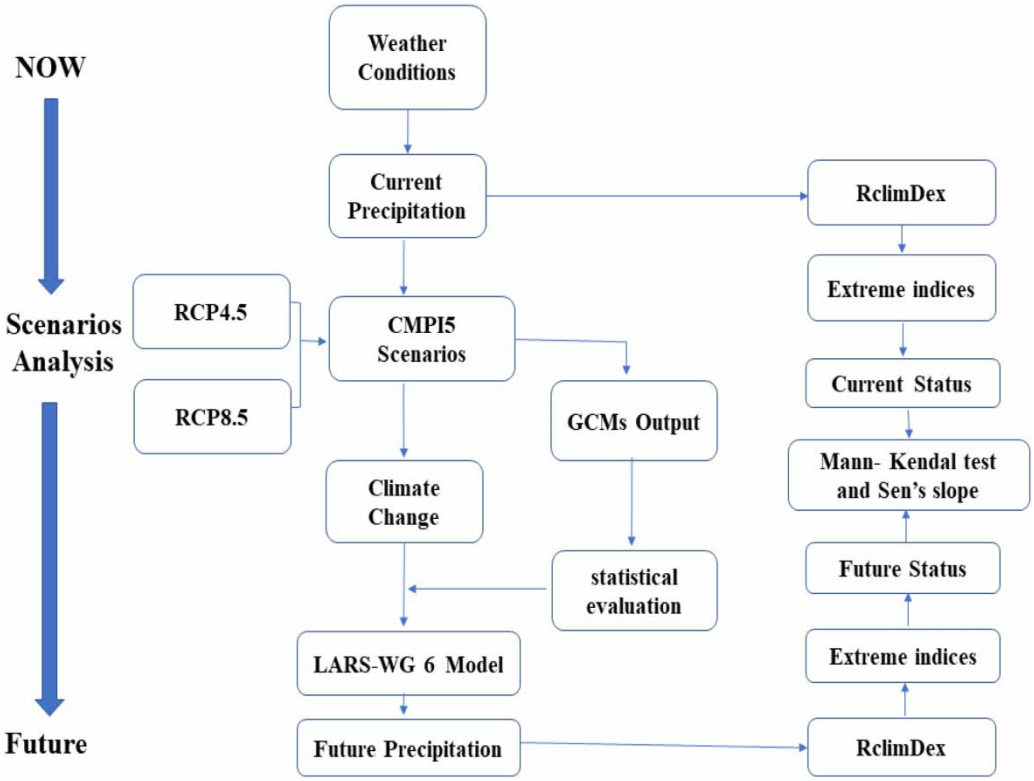

Figure 2 | The general flowchart of the methodology.

Table 3 | Definitions of the used precipitation indices

Index	Descriptive name	Units
PRCPTOT	Wet-day precipitation	mm
RX1day	Maximum 1-day precipitation	mm
RX5day	Maximum 5-day precipitation	mm
R95	Very wet day	mm
R99	Extreme very wet day	mm
SDII	Simple daily intensity index	mm/d
CWD	Consecutive wet days	day
CDD	Consecutive dry days	day

$$\mathrm{sgn}(x_j - x_i) = \begin{cases} +1 & \text{if} \quad (x_j - x_i) > 0 \\ 0 & \text{if} \quad (x_j - x_i) = 0 \\ -1 & \text{if} \quad (x_j - x_i) < 0 \end{cases} \tag{7}$$

The variance of S is calculated by Equation (8):

$$\mathrm{Var}(S) = \frac{n(n-1)(2n+5) - \sum_{i=1}^{k} t_i(t_i-1)(t_i+5)}{18}, \tag{8}$$

where k is the tied groups representing observations having the same value, and t_i is the number of values of the ith group. The standardized MK statistic (Z) is calculated by Equation (9):

$$Z = \begin{cases} \dfrac{S-1}{\sqrt{\mathrm{var}(S)}} & \text{if} \quad S > 0 \\ 0 & \text{if} \quad S = 0 \\ \dfrac{S+1}{\sqrt{\mathrm{var}(S)}} & \text{if} \quad S < 0 \end{cases} \tag{9}$$

The statistic Z follows the standard normal distribution. If the Z statistic is positive, the trend of the data series will be upward, and if it is negative, the trend will be decreasing.

In addition, the Sen's estimator was used to estimate the actual trend slope (β) in the time series. This method calculates the overall slope using the median of the slopes of all the pairs of sequential data (X_j and X_i). The estimate is expressed as follows:

$$\beta = \mathrm{Median}\left[\frac{X_j - X_i}{j-i}\right] \quad \text{for all} \quad j > i \tag{10}$$

3. RESULTS AND DISCUSSION

3.1. Validation of selected CMIP5 models

The performance evaluation and comparison of the proposed models are reported in Table 4. The results showed that HadGEM2-ES, GFDL-CM3, NorESM1-M, and MIROC5 models have a high correlation with the observed precipitation in the basin. The results showed that based on the error statistics (RMSE, MAE, MBE, and MPE) and R^2, HadGEM2-ES, GFDL-CM3, NorESM1-M, and MIROC5 models are the most suitable models for the Lake Urmia basin. In terms of the MPE, these models have the lowest error percentage (between 9 and 12%). Positive values of MBE indicate an overestimation of GCMs, and its negative values indicate an underestimation of these models. Therefore, these four models were used to create the ensemble model and to investigate precipitation changes.

3.2. Evaluation of the results of LARS-WG

The outputs of the LARS-WG 6.0 downscaling method compared with the observed values are shown in Figure 3. The results of the LARS-WG evaluation show that the overall performance of the method was very good. There is a high similarity between the observed and modeled values for the mean monthly precipitation. Similar results were obtained by Goudarzi *et al.* (2015) and Lotfi *et al.* (2022). On the basis of this ability of LARS-WG to capture mean monthly precipitation (Figure 3), we applied this method for predicting future precipitation for the basin.

The adequacy of the LARS-WG model to predict the precipitation was tested using the p-value of the Kolmogorov–Smirnov (K-S) test. The K-S test is performed to check the equality of the seasonal distributions of wet and dry series and distributions

Table 4 | The accuracy evaluation of GCM simulated precipitation in the lake Urmia Basin (1987–2016)

Model	R2	RMSE	MAE	MBE	MPE	Model	R^2	RMSE	MAE	MBE	MPE
BCC-CSM1.1	0.29	16.02	23.77	23.34	21.28	IPSL-CM5A-MR	0.22	16.68	20.62	20.62	18.76
CanESM2	0.38	13.55	19.09	19.09	17.78	**MIROC5**	**0.53**	**10.16**	**12.64**	**11.66**	**11.02**
CNRM-CM5	0.32	14.55	18.25	−6.19	16.89	MIROC-ESM	0.46	12.26	16.65	16.65	14.51
CSIRO-MK36	0.32	15.17	22.71	22.25	20.09	MPI-ESM-MR	0.52	11.24	14.31	12.49	12.51
EC-EARTH	0.52	10.74	15.08	14.81	12.50	MRI-CGCM3	0.50	11.76	15.89	10.84	14.33
GFDL-CM3	**0.58**	**9.10**	**10.70**	**− 9.66**	**9.01**	NCAR-CCSM4	0.37	14.05	19.85	19.15	17.65
GISS-E2-R-CC	0.41	12.98	17.50	9.48	19.72	NCAR-CESM1-CAM5	0.14	17.50	21.72	−11.1	19.41
HadGEM2-ES	**0.62**	**8.14**	**11.81**	**10.58**	**10.49**	**NorESM1-M**	**0.55**	**9.62**	**13.47**	**11.16**	**12.01**

Note: Models with bold value have a best performance than other models.

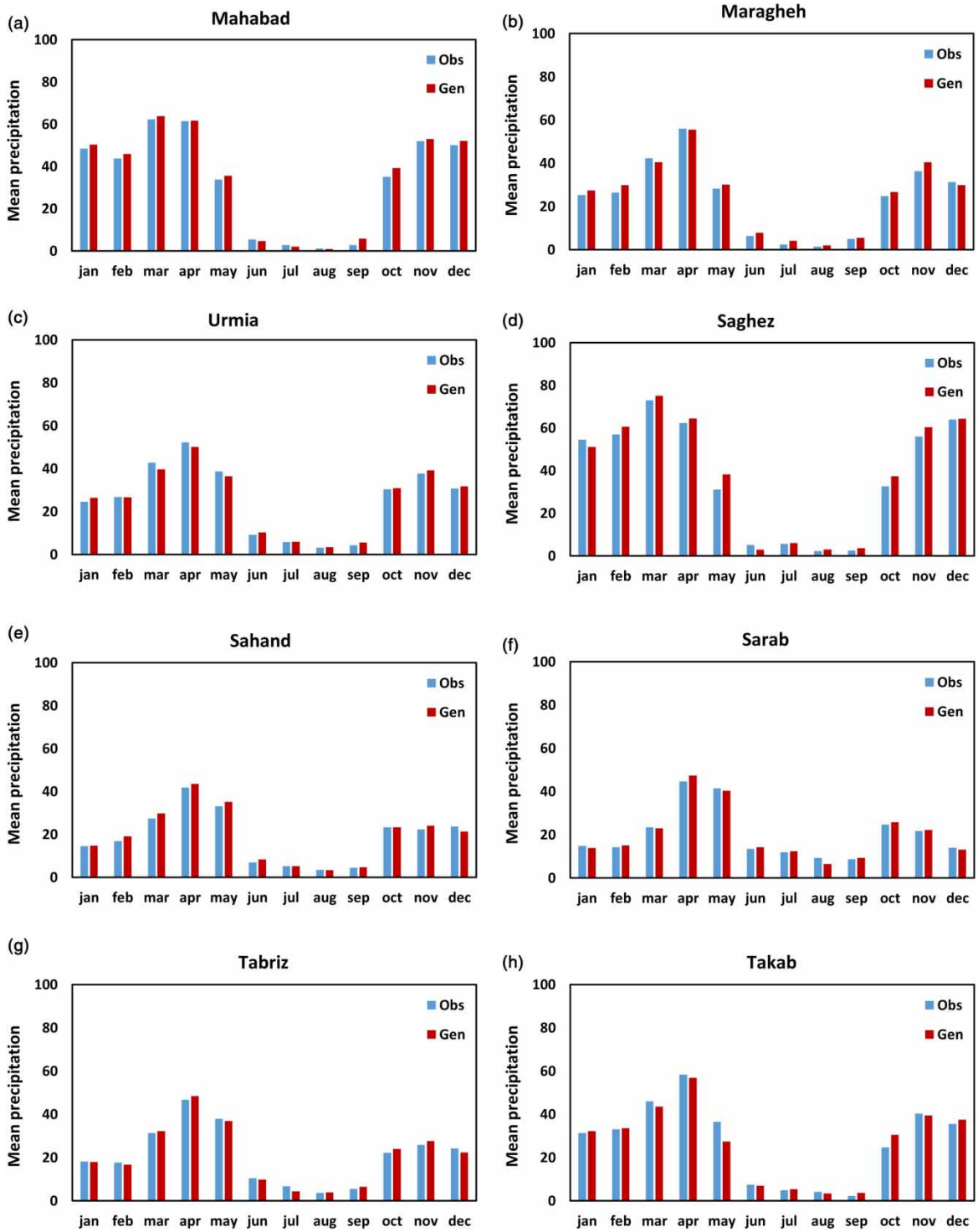

Figure 3 | Observed and generated mean monthly precipitation for eight stations in the Lake Urmia basin for the period 1987–2016.

of daily rainfall calculated from observed data and downscaled data (Wilks 2011). This test calculates a *p*-value, which is used to accept or reject the hypotheses that two datasets could have come from the same distribution (i.e., when there is no difference between the observed and predicted data). A very low *p*-value means the predicted data are unlikely to be the same as

the observed data and hence should be rejected. The results of the K-S (Kolmogorov–Smirnov) test show that there was no significant difference between the distributions of the daily observed and modeled series for all weather stations. The acceptable *p*-value from the LARS-WG manual is more than 0.01 (Semenov & Barrow 2002). In most months, the *p*-values are above this range, indicating that the data follow a normal distribution (Table 5). The LARS-WG model was thus judged to be acceptable to generate synthetic weather series based on projected climate scenarios.

3.3. Precipitation changes in the reference period and the future period

By calibrating the LARS-WG model and ensuring its ability to optimally simulate precipitation data series, this model was implemented for predicting the future climate of the period 2021–2100, using the output of the ensemble model based on RCP4.5 and RCP8.5. The temporal variations of the mean annual precipitation in the base period and the future are shown in Figure 4. In the base period, the annual precipitation shows a decreasing trend but is not significant. In the future period, both scenarios show decreasing trends (Figure 4). The trend slope in the RCP8.5 scenario is higher than RCP4.5. Precipitation decreasing in the Lake Urmia basin is also reported by Bashirian *et al.* (2020). Their results indicated that the frequency of droughts increased, and annual precipitation decreased during 1961–2017.

In general, it can be said that in the base period, in January, February, March, April, June, August, and December, there is a decreasing trend (Table 6). Moreover, in May, July, September, October, and November, there is an increasing trend in precipitation. In the coming periods and in January, April, May, June, July, August, November, and December, a decreasing trend is observed. In February, March, September, and October, an increasing trend is observed in the basin. However, the trend slope based on RCP8.5 is higher than RCP4.5.

The results of previous studies also show a decrease in precipitation in future periods in Iran and the Lake Urmia basin (Sayadi *et al.* 2019; Motiee *et al.* 2020; Davarpanah *et al.* 2021). This result is consistent with the results presented in the

Table 5 | *P*-values from the K-S test for daily rainfall distribution for each month over eight stations in Iran

Station	Jan	Feb	Mar	Apr	May	Jun	Jul	Aug	Sep	Oct	Nov	Dec
Mahabad	1	1	1	0.98	0.99	0.97	0.21	0.84	0.09	1	0.98	1
Maragheh	1	1	1	0.98	0.99	0.97	0.21	0.84	0.09	1	0.98	1
Urmia	1	1	1	1	1	1	0.63	0.00	1	1	0.99	1
Saghez	1	1	1	1	1	1	0.35	0.30	0.49	1	1	1
Sahand	1	1	1	1	1	1	1	1	1	1	.99	1
Sarab	1	1	1	1	1	0.99	0.99	0.96	0.85	0.92	1	1
Tabriz	1	1	1	1	1	0.97	0.99	0.62	1	0.95	0.99	1
Takab	0.99	1	1	1	0.99	0.97	0.49	0.96	0.09	1	.80	1

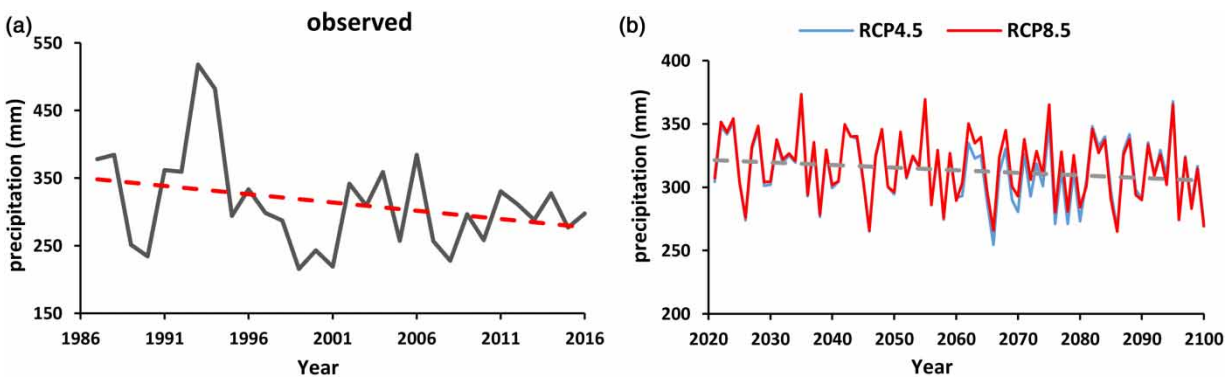

Figure 4 | Changes of annual precipitation based on (a) observed data and (b) projected data under RCP4.5 and RCP8.5 scenarios.

Table 6 | The mean value of annual precipitation (P/mm), Mann–Kendall test values (Z), and Sen's slope (S) in the base period (1987–2016) and in the future period (2021–2100)

Time scale	Value	Observed	RCP4.5	RCP8.5
January	P	30.34	33.4	32.42
	Z	−0.71	−0.31	−0.38
	Slope	−0.247	−0.009	−0.010
February	P	29.81	34.8	33.9
	Z	−1.75	2.27*	1.52
	Slope	−0.552	0.088	0.057
March	P	43.83	49.7	48.8
	Z	−1.86	1.08	0.44
	Slope	−0.620	0.069	0.023
April	P	53.86	49	48.5
	Z	−0.96	−2.56**	−2.96**
	Slope	−0.506	−0.146	−0.175
May	P	34.30	26.1	26.3
	Z	0.21	−6.24**	−6.58**
	Slope	0.168	−0.189	−0.207
June	P	8.22	7.9	8
	Z	−0.21	−1.95	−2.41*
	Slope	−0.019	−0.030	−0.039
July	P	5.49	6.6	6.8
	Z	0.27	−3.15**	−3.11**
	Slope	0.014	−0.046	−0.049
August	P	3.51	2.5	2.7
	Z	−0.12	−1.25	−0.91
	Slope	−0.003	−0.009	−0.008
September	P	4.49	8.1	9.4
	Z	1.53	5.52**	5.60**
	Slope	0.075	0.108	0.131
October	P	27.43	27.5	30.5
	Z	0.00	1.76	2.77**
	Slope	0.015	0.056	0.090
November	P	37.22	32.5	34
	Z	0.46	−0.77	0.28
	Slope	0.186	−0.024	0.010
December	P	34.24	35.1	34.8
	Z	−0.29	−0.25	0.29
	Slope	−0.104	−0.012	0.009
Annual	P	312.74	313.3	316.2
	Z	−1.25	−1.72	−1.87
	Slope	−2.075	−0.234	−0.238

*Trend at 95% confidence level.
**Trend at a 99% confidence level.

study by Abbasian *et al.* (2021), who showed an 8% decrease in precipitation in 2060–2080 based on RCP8.5. Naderi & Saatsaz (2020) also reported a decrease of 10% in annual precipitation.

3.4. Changes in extreme indices in the base period and the future period

Changes in absolute precipitation indices in the reference and the future period are shown in Figure 5. In the baseline period, Rx1day and Rx5day in the baseline period (1987–2016) have a decreasing trend. The highest RX1day index occurred in 1991. The rate of decrease of this index in the basin is about 1.1 mm per decade. The highest rate of the RX5day index occurred in 1994, and its average decrease is 2.1 mm per decade. According to RCP4.5, the Rx1day and Rx5day indices are expected to

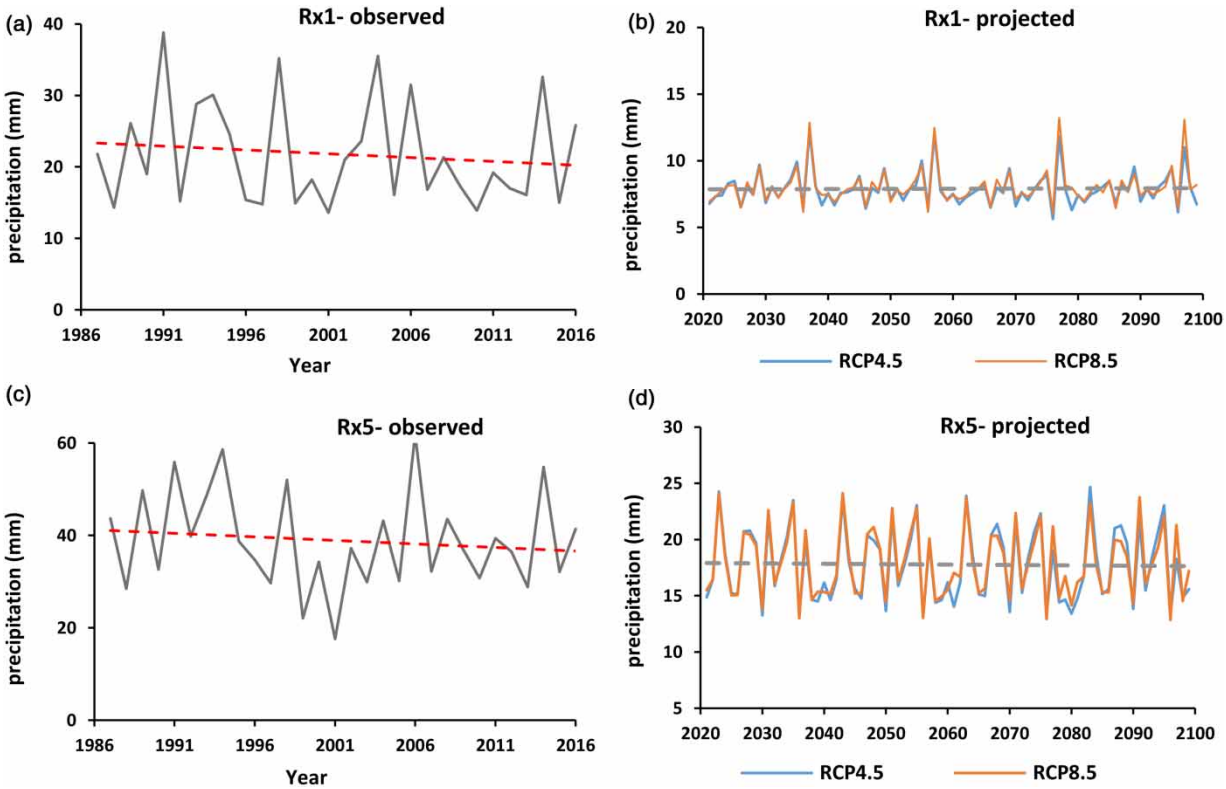

Figure 5 | Comparison of the absolute precipitation indices over (a and c) the base period and (b and d) the future periods based on RCP4.5 and RCP8.5 scenarios.

decrease in the period 2021–2100, which will be more than 50% compared to the reference period. Also based on the RCP8.5, the value of Rx1day and Rx5day indices decreases, which is on average more than 10 mm compared to the baseline period.

Because Rx1day and Rx5day indices indicate the continuity of cyclonic systems or instability in 1-day and multiday periods, they are suitable indicators for the flood study. Considering that the amount of these indices will decrease in the future in the Lake Urmia basin, it can be concluded that the potential for floods and the resulting damage in the region will be reduced. Fathian *et al.* (2022) obtained similar results on the behaviors of changes in RX1day and RX5day.

Table 7 shows the results of the trend test and the slope estimates of the predicted indices based on the RCP4.5 and RCP8.5. Rx1day has an upward trend, whereas Rx5day has a downward trend based on both scenarios, but the trends of the indicators are not significant. Zarrin & Dadashi-Roudbari (2021) reported an increasing trend in Rx1day, which is consistent with the results of this study.

Changes in percentile precipitation indices in the reference period and the future period are shown in Figure 6. R95p and R99p have a decreasing trend in the baseline period, but this trend is not significant. In the next period, based on both RCP4.5 and RCP8.5 scenarios, R95p will decrease compared to the baseline period, but R99p will increase.

The overall rate of R95p based on RCP4.5 and RCP8.5 scenarios for the Lake Urmia basin is −2.7 and −0.4 mm per decade, respectively. The overall rate of R99p based on RCP4.5 and RCP8.5 is 0.2 and 2.7 mm per decade, respectively (Table 7). Darand (2020) and Soltani *et al.* (2020) reported an increase in the heavy rainfall over Iran in the future. Fathian *et al.* (2022) showed that the number of stations with a positive trend in R95p will increase in the future in Iran. However, most stations situated in the north and northwest regions show negative trends that are in agreement with our findings.

Figure 7 shows the changes in periodic indices in the reference period and the future. During the baseline period, the CDD decreased to about 4.6 days per decade. The highest number of dry days was 138 in 1990, and the lowest number of days was 28 in 2011. The CWD in the baseline period increased slightly, but in the next period, the CWD showed a decreasing trend, which is not significant based on both scenarios. It is predicted that in future periods, the CDD index will increase in both scenarios (Figure 7). This index has a significant upward trend for RCP4.5 and RCP8.5 scenarios, with a slope of about 1.7

Table 7 | M-K statistic and Sen's slope for extreme precipitation indices in the reference period and the future period based on RCP4.5 and RCP8.5 scenarios

Index	Trend	Observed	RCP4.5	RCP8.5
Rx1day	Z	−0.45	0.45	0.83
	Slope	−0.089	0.002	0.004
Rx5day	Z	−0.68	−0.16	−0.07
	Slope	−0.150	−0.001	−0.002
R95p	Z	−0.36	−0.44	−0.05
	Slope	−0.027	−0.027	−0.004
R99p	Z	−0.96	0.39	0.94
	Slope	0.00	0.002	0.027
CDD	Z	−0.80	2.28*	2.65*
	Slope	−0.278	0.172	0.179
CWD	Z	0.52	−0.34	−0.49
	Slope	0.00	0.00	0.00
PRCPTOT	Z	−1.25	−1.37	−1.66
	Slope	−2.438	−0.196	−0.215
SDII	Z	−1.45	−0.67	−0.41
	Slope	−0.023	0.00	0.00

*Trend at a 99% confidence level.

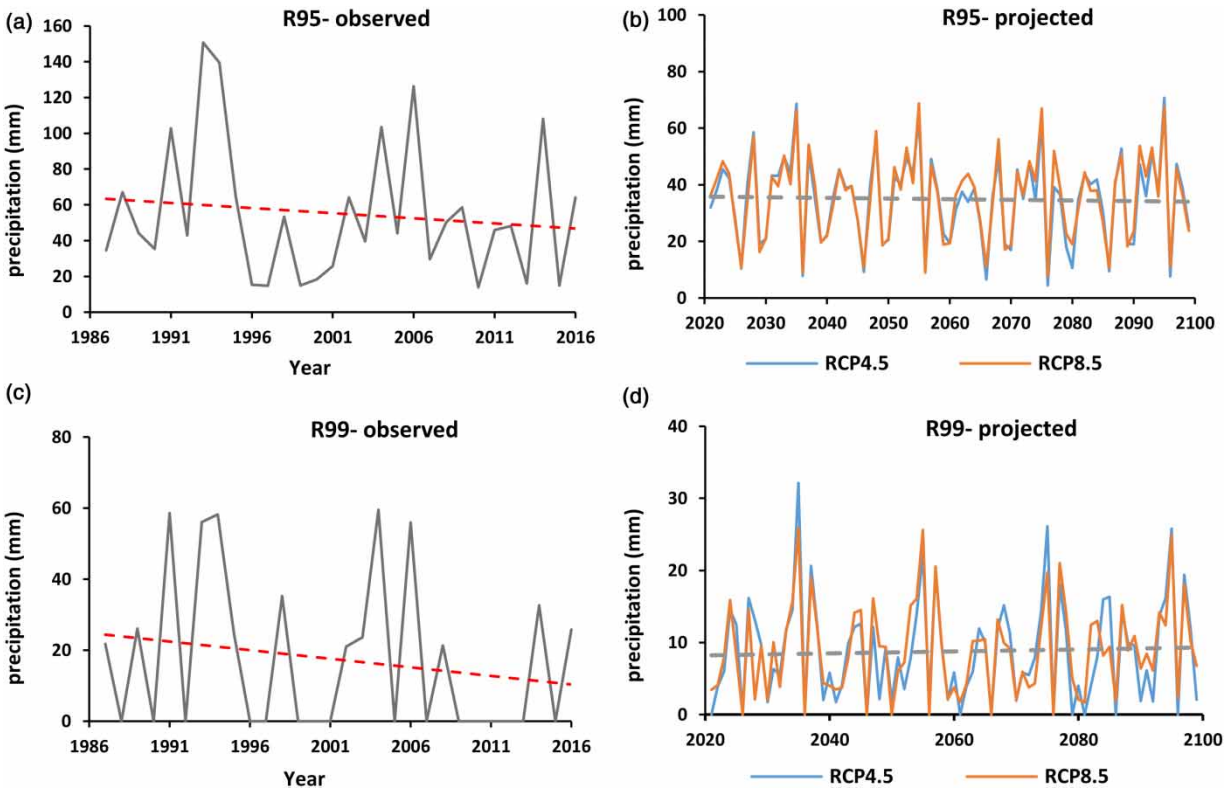

Figure 6 | Comparison of the percentile precipitation indices over (a and c) the base period and (b and d) the future periods based on RCP4.5 and RCP8.5 scenarios.

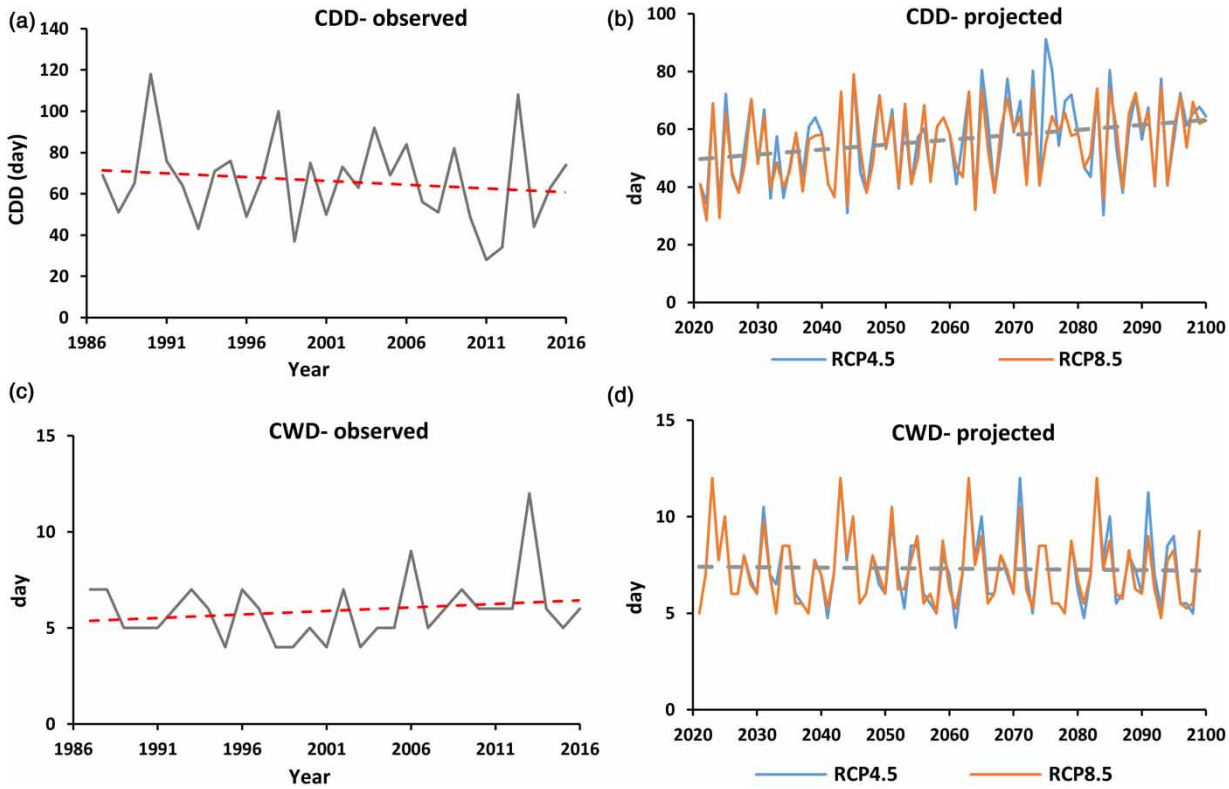

Figure 7 | Comparison of the duration precipitation indices over (a and c) the base period and (b and d) the future periods based on RCP4.5 and RCP8.5 scenarios.

and 1.8 days per decade, respectively (Table 7). Therefore, it can be said that the Lake Urmia basin will see drier climatic conditions in the future. Darand (2020) showed the increase of CDD in Iran, especially in the northwest in the future period. Zarrin *et al.* (2022) also reported that CDD in Iran will increase by a maximum of 26.4 days in the period 2061–2100 under the SSP5-8.5 scenario for the Caspian Sea and Lake Urmia basins, and CWD will decrease in these two basins.

Changes in PRCPTOT and SDII indices in the base and future periods are shown in Figure 8. PRCPTOT shows that during the reference period, the precipitation trend is decreasing. On average, during the period 1987–2016, the total annual precipitation decreased by about 24 mm per decade. The SDII also decreased in the baseline period, but the amount of this decrease is insignificant. In the future period, the PRCPTOT will decrease for both scenarios. According to the RCP4.5 scenario, a decreasing trend is observed with a slope of 1.9 mm per decade. A similar downward trend in the RCP8.5 scenario is predicted with a slope of about 2.1 mm per decade.

The results of downscaling based on RCP4.5 and RCP8.5 in the Lake Urmia Basin show insignificant changes in SDII in all three periods (Figure 8(c)). Examining the trend of this index also shows a downward trend in both scenarios, but the slope of this trend is small (Table 7). Darand (2020) showed that annual total precipitation decreased in the future period, and the projected decreases were larger in the northwestern parts of Iran.

To accurately study the trend of future precipitation indices, the trends with a width of 20-year periods (2021–2040, 2041–2060, 2061–2080, and 2081–2100) were calculated and compared with the trend of the baseline period (Figure 9). The RX1day, R99p, and CDD have a decreasing trend in the baseline period but have an increasing trend in future periods in both scenarios. RX5day, R95p, PRCPTOT, and SDII have a declining trend in both the reference and future periods except for R95p in the period 2041–2060. Although the CWD has an increasing trend in the reference period, it has a decreasing trend in future periods based on RCP4.5 and RCP8.5.

3.5. Limitations

There are a few limitations to this study. First, the number of synoptic stations in Iran, especially in the Lake Urmia basin, is very low and scattered, and most of the stations are newly established and their period is short. As a result, the zoning of

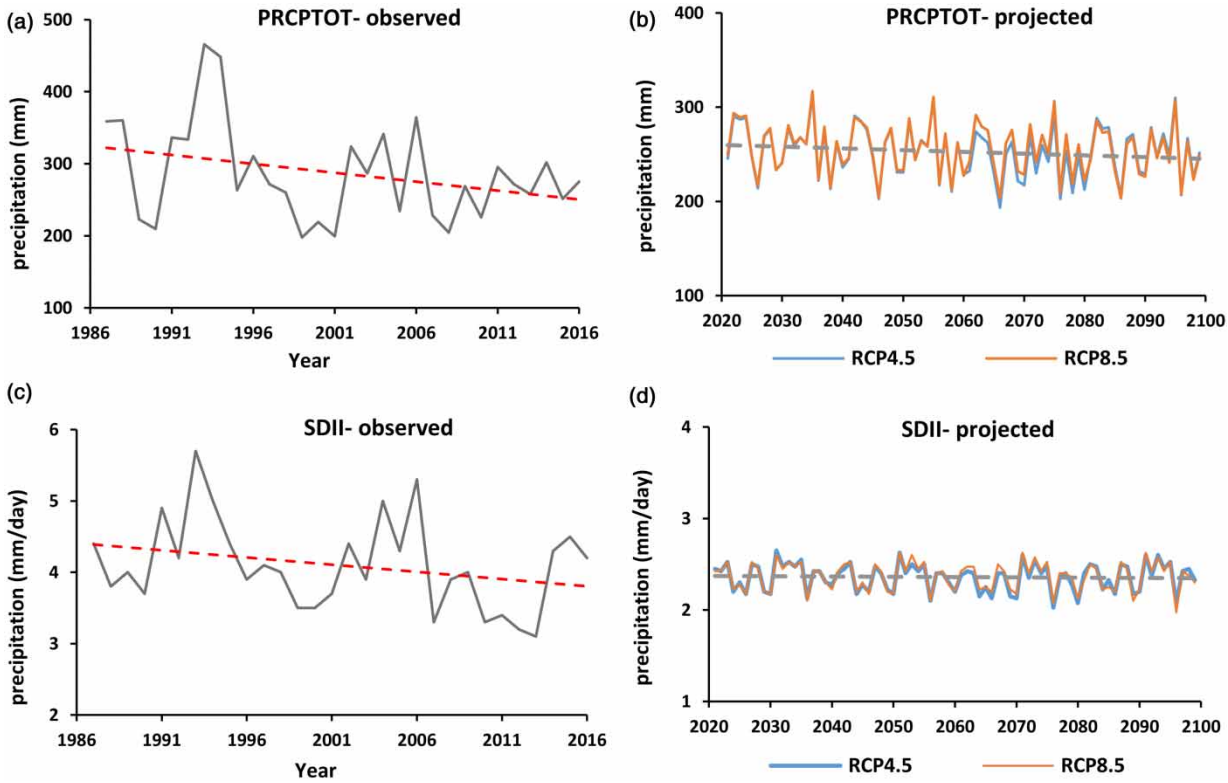

Figure 8 | Comparison of PRCPTOT and SDII over (a and c) the base period and (b and d) the future periods based on RCP4.5 and RCP8.5 scenarios.

climatic variables and extreme indicators in the basin is difficult. Furthermore, the ETCCDI indices are defined generally at annual timescales, and some are defined at monthly timescales as well. For some sectoral applications (e.g., in agriculture water resource management and energy), the current set of monthly/annual indices may prove less helpful, as climate anomalies need to be computed over different timescales. Thus, the results of this study are subject to some uncertainties in the prediction of precipitation and especially in extreme values (Najafi & Hesami Kermani 2017; Hong *et al.* 2022). We may need to employ other statistical methods such as based on return level estimation (EskandariPour & Soltaninia 2022; Rivoire *et al.* 2022).

4. CONCLUSION

This study was conducted to provide a perspective on future changes in precipitation extreme indices in the Lake Urmia Basin in the period 2021–2100. For this purpose, the output of 16 GCMs was examined. HadGEM2, GFDL, NorESM1, and MIROC5 models were selected as suitable models for the basin. The output of these four models was downscaled by LARS-WG. Then, an ensemble model was created by model averaging. Finally, precipitation extreme indices were calculated for the studied stations, and then the regional average for the whole basin was obtained. By comparing the changes in precipitation between the reference period and the future, we obtained a conclusion that the average precipitation of the basin in the future period will decrease in both scenarios.

The results also showed that the number of CDDs will increase with a possible decrease in precipitation during the next period. This can be considered as a drought potential index and based on increasing greenhouse gases (Sillmann *et al.* 2013). Other indices (Rx1day, Rx5day, R95p, R99p, CWD, SDII, and PRCPTOT) based on both scenarios are reduced compared to the baseline period. In the Lake Urmia basin, there is a positive and negative relationship between the increase in rainfall with the rate of CWD and CDD, respectively, which has been confirmed by many studies in other regions of the world (Sharma *et al.* 2020; Wang *et al.* 2021). Also, the slope of significant trends in RCP8.5 is higher than in RCP4.5.

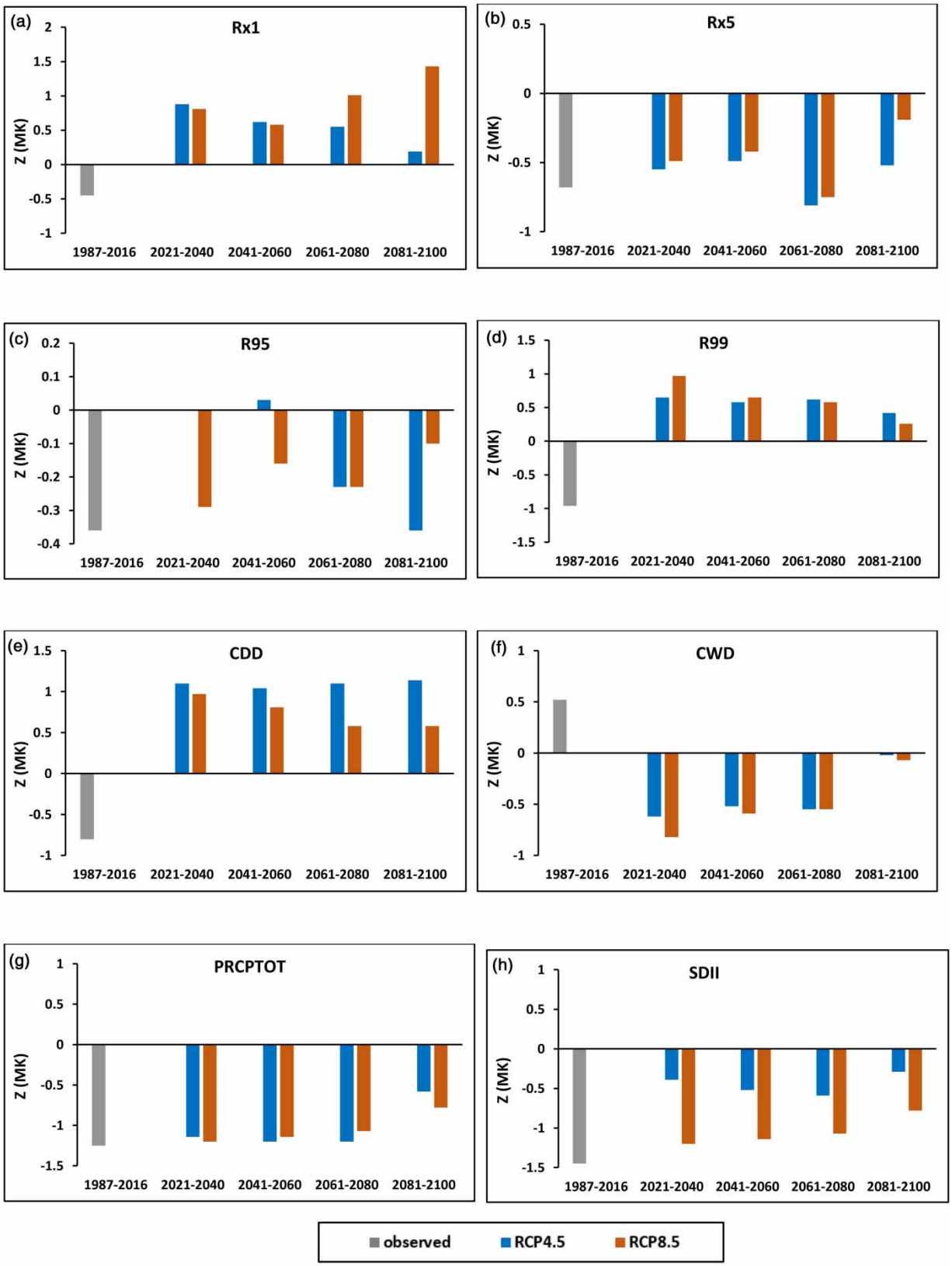

Figure 9 | (a–h) Mann–Kendall test values in the base period (1987–2016) and the future subperiods based on RCP4.5 and RCP8.5 scenarios.

The results of this study have important implications for the management of water resources in climate change conditions. Increasing the frequency of CDDs, decreasing precipitation, and decreasing wet days may make the soil drier. This may induce a serious effect on the hydrological cycle. Also, the increase in frequent dry periods causes a decrease in soil fertility, which in turn causes a decrease in agricultural production. Moreover, the decrease in agriculture and the ever-increasing population growth may pose a serious threat to food security in the Lake Urmia basin, which is the agricultural pole of Iran. Therefore, it is necessary to implement comprehensive policies to prepare for future water shortages in the basin, by quantifying the amount of precipitation decrease and temperature increase.

ACKNOWLEDGEMENTS

The authors are grateful to the Editor and to the reviewers for their valuable and constructive comments. We also gratefully acknowledge the project funding provided by Urmia Lake Research Institute, Urmia University, Iran. The work by Park was supported by the National Research Foundation of Korea (No. 2020R1I1A3069260).

DATA AVAILABILITY STATEMENT

Data cannot be made publicly available; readers should contact the corresponding author for details.

CONFLICT OF INTEREST

The authors declare there is no conflict.

REFERENCES

Abbasi, A., Amirabadizadeh, M., Afshar, A. A. & Yaghoobzadeh, M. 2022 Potential influence of climate and land-use changes on green water security in a semi-arid catchment. *J. Water Clim. Change* **13** (1), 287–303.

Abbasian, M. S., Najafi, M. R. & Abrishamchi, A. 2021 Increasing risk of meteorological drought in the Lake Urmia basin under climate change: introducing the precipitation–temperature deciles index. *J. Hydrol.* **592**, 125586.

Abbaspour, M., Javid, A. H., Mirbagheri, S. A., Givi, F. A. & Moghimi, P. 2012 Investigation of lake drying attributed to climate change. *Int. J. Environ. Sci. Technol.* **9**, 257–266.

AghaKouchak, A., Norouzi, H., Madani, K., Mirchi, A., Marzi Azarderakhsh, M., Nazemi, A., Nasrollahi, N., Farahmand, A., Mehran, A. & Hasanzadeh, E. 2015 Aral sea syndrome desiccates Lake Urmia: call for action. *J. Great Lakes Res.* **41**, 307–311.

Alexander, L. V., Zhang, X., Peterson, T. C., Caesar, J., Kumar, K., Gleason, B., Klein Tank, A. MG., Collins, D., Trewin, B., Rahimzadeh, F., Tagipour, A., Kumar, R. K., Revadekar, J., Georgina, G., Vincent, L., Stephenson, D. B., Burn, J., Aguilar, E., Brunet, M., Taylor M, Zhai P., Rusticucci M. & Vazquez-Aguirre J. L. 2006 Global observed changes in daily climate extremes of temperature and precipitation. *J. Geophys. Res. Atmos.* **111**, 1–22.

Aloysius, N. R., Sheffield, J., Saiers, J. E., Li, H. & Wood, E. F. 2016 Evaluation of historical and future simulations of precipitation and temperature in Central Africa from CMIP5 climate models. *J. Geophys. Res. Atmos.* **121**, 130–152.

Ashktorab, N. & Zibaei, M. 2022 Future virtual water flows under climate and population change scenarios: focusing on its determinants. *J. Water Clim. Change* **13** (1), 96–112.

Azizzadeh, M. & Javan, K. 2018 Temporal and spatial distribution of extreme precipitation indices over the lake Urmia Basin, Iran. *Environ. Resour. Res.* **6**, 25–40.

Bashirian, F., Rahimi, D., Movahedi, S. & Zakerinejad, R. 2020 Water level instability analysis of Urmia Lake Basin in the northwest of Iran. *Arabian J. Geosci.* **13** (4), 1–14.

Darand, M. 2020 Projected changes in extreme precipitation events over Iran in the 21st century based on CMIP5 models. *Clim. Res.* **82**, 75–95.

Davarpanah, S., Erfanian, M. & Javan, K. 2021 Assessment of climate change impacts on drought and wet spells in Lake Urmia Basin. *Pure Appl. Geophys.* **178**, 545–563.

Delju, A. H., Ceylan, A., Piguet, E. & Rebetez, M. 2013 Observed climate variability and change in Urmia Lake Basin, Iran. *Theor. Appl. Climatol.* **111**, 285–296.

Esa, A. I. M., Halim, S. A., Ali, N., Chung, J. X. & Mohd, M. S. F. 2022 Optimizing future mortality rate prediction of extreme temperature-related cardiovascular disease based on skewed distribution in peninsular Malaysia. *J. Water Clim. Change* **13** (11), 3830–3850.

EskandariPour, M. & Soltaninia, S. 2022 Analyzing the duration frequency and severity of drought using copula function in the Yazd city. *J. Water Clim. Change* **13** (1), 67–82.

Fathian, F., Ghadami, M., Haghighi, P., Amini, M., Naderi, S. & Ghaedi, Z. 2020 Assessment of changes in climate extremes of temperature and precipitation over Iran. *Theor. Appl. Climatol.* **141**, 1119–1133.

Fathian, F., Ghadami, M. & Dehghan, Z. 2022 Observed and projected changes in temperature and precipitation extremes based on CORDEX data over Iran. *Theor. Appl. Climatol.* **149**, 569–592.

Fuhrer, J. 2003 Agroecosystem responses to combinations of elevated CO_2, ozone, and global climate change. *Agric. Ecosyst. Environ.* **97**, 1–20.

Goudarzi, M., Salahi, B. & Hosseini, S. A. 2015 Performance assessment of LARS-WG and SDSM downscaling models in simulation of climate changes in Urmia Lake Basin. *Iran-Watershed Manage. Sci. Eng.* **9**, 11–23.

Graham, L. P., Hagemann, S., Jaun, S. & Beniston, M. 2007 On interpreting hydrological change from regional climate models. *Clim. Change* **81**, 97–122.

Grover, S., Tayal, S., Sharma, R. & Beldring, S. 2022 Effect of changes in climate variables on hydrological regime of Chenab basin, western Himalaya. *J. Water Clim. Change* **13** (1), 357–371.

Hong, J., Javan, K., Shin, Y. & Park, J. S. 2021 Future projections and uncertainty assessment of precipitation extremes in Iran from the CMIP6 ensemble. *Atmos* **12** (8), 1052.

Hong, J., Agustin, W., Yoon, S. & Park, J. S. 2022 Changes of extreme precipitation in the Philippines, projected from the CMIP6 multi-model ensemble. *Weather Clim. Extremes* **37**, 100480.

Hu, Y., Maskey, S. & Uhlenbrook, S. 2012 Trends in temperature and rainfall extremes in the Yellow River source region, China. *Clim. Change* **110**, 403–429.

IPCC 2013 Climate Change 2013: The Physical Science Basis. In: *Contribution of Working Group I to the Fifth Assessment Report of the Intergovernmental Panel on Climate Change* (Stocker, T. F., ed.). Cambridge University Press, Cambridge, p. 1552.

Kavwenje, S., Zhao, L., Chen, L. & Chaima, E. 2022 Projected temperature and precipitation changes using the LARS-WG statistical downscaling model in the Shire River Basin, Malawi. *Int. J. Climatol.* **42** (1), 400–415.

Khazaei, B., Khatami, S., Alemohammad, S. H., Rashidi, L., Wu, C., Madani, K., Kalantari, Z., Destouni, G. & Aghakouchak, A. 2019 Climatic or regionally induced by humans? Tracing hydro-climatic and land-use changes to better understand the Lake Urmia tragedy. *J. Hydrol.* **569**, 203–217.

Kilsby, C. G., Jones, P. D., Burton, A., Ford, A. C., Fowler, H. J., Harpham, C., James, P., Smith, A. & Wilby, R. L. 2007 A daily weather generator for use in climate change studies. *Environ. Modell. Software* **22**, 1705–1719.

Lee, Y., Shin, Y., Boo, K. O. & Park, J. S. 2020 Future projections and uncertainty assessment of precipitation extremes in the Korean peninsula from the CMIP5 ensemble. *Atmos. Sci. Lett.* **21** (2), e954.

Liu, L., Liu, Z., Ren, X., Fischer, T. & Xu, Y. 2011 Hydrological impacts of climate change in the Yellow River Basin for the 21st century using hydrological model and statistical downscaling model. *Quat Int.* **244**, 211–220.

Lotfi, M., Kamali, G. A., Meshkatee, A. H. & Varshavian, V. 2022 Performance analysis of LARS-WG and SDSM downscaling models in simulating temperature and precipitation changes in the West of Iran. *Model. Earth Syst. Environ.* **111**, 1–11. https://www.rothamsted.ac.uk/lars-wg-weather-simulation-model.

Moss, R. H., Edmonds, J. A., Hibbard, K. A., Manning, M. R., Rose, S. K., van Vuuren, D. P., Carter, T. R., Emori, S., Kainuma, M., Kram, T., Meehl, G. A., Mitchell, J. F., Nakicenovic, N., Riahi, K., Smith, S. J., Stouffer, R. J., Thomson, A. M., Weyant, J. P. & Wilbanks, T. J. 2010 The next generation of scenarios for climate change research and assessment. *Nature* **463**, 747.

Motiee, H., McBean, E., Motiee, A. R. & Majdzadeh Tabatabaei, M. R. 2020 Assessment of climate change under CMIP5-RCP scenarios on downstream rivers glaciers–Sardabrud River of Alam-Kuh Glacier, Iran. *Int. J. River Basin Manage.* **18**, 39–47.

Naderi, M. & Saatsaz, M. 2020 Impact of climate change on the hydrology and water salinity in the Anzali Wetland, northern Iran. *Hydro. Sci. J.* **65** (4), 552–570.

Najafi, R. & Hesami Kermani, M. R. 2017 Uncertainty modeling of statistical downscaling to assess climate change impacts on temperature and precipitation. *Water Resour. Manage.* **31**, 1843–1858.

Rahimzadeh, F., Asgari, A. & Fattahi, E. 2009 Variability of extreme temperature and precipitation in Iran during recent decades. *Int. J. Climatol.* **29** (3), 329–343.

Reddy, K. S., Kumar, M., Maruthi, V., Umesha, B., Vijayalaxmi & Nageswar Rao, C. V. K. 2014 Climate change analysis in southern Telangana region, Andhra Pradesh using LARS-WG model. *Curr. Sci.* **107**, 54–62.

Rivoire, P., Le Gall, P., Favre, A.-C., Naveau, P. & Martius, O. 2022 High return level estimates of daily ERA-5 precipitation in Europe estimated using regionalized extreme value distributions. *Weather Clim. Extremes* **38**, 100500.

Sayadi, A., Beydokhti, N. T., Najarchi, M. & Najafizadeh, M. M. 2019 Investigation into the effects of climatic change on temperature, rainfall, and runoff of the Doroudzan catchment, Iran, using the ensemble approach of CMIP3 climate models. *Adv. Meteorol.* **1**, 1–16.

Semenov, M. A. & Barrow, E. M. 2002 LARS-WG, A stochastic weather generator for use in climate impact studies. User Man. Rothamsted Research, Herts, Harpenden, UK, 1–27.

Semenov, M. A. & Stratonovitch, P. 2010 Use of multi-model ensembles from global climate models for assessment of climate change impacts. *Clim. Res.* **41**, 1–14.

Sharma, S., Khadka, N., Hamal, K., Baniya, B., Luintel, N. & Joshi, B. B. 2020 Spatial and temporal analysis of precipitation and its extremities in seven provinces of Nepal (2001–2016). *Appl. Ecol. Environ. Sci.* **8** (2), 64–73.

Sillmann, J., Kharin, V. V., Zwiers, F. W., Zhang, X. & Bronaugh, D. 2013 Climate extremes indices in the CMIP5 multimodel ensemble: part 2. Future climate projections. *J. Geophys. Res. Atmos.* **118**, 2473–2493.

Soltani, M., Laux, P., Kunstmann, H., Stan, K., Sohrabi, M. M., Molanejad, M., Sabziparvar, A. A., SaadatAbadi, A. R., Ranjibar, F., Rousta, I., Zawar-Reza, P., Khoshakhlagh, F., Soltanzadeh, I., Babu, C. A., Azizi, G. H. & Martin, M. V.2016 Assessment of climate variations in temperature and precipitation extreme events over Iran. *Theor. Appl. Climatol.* **126**, 775–795.

Soltani, S., Almasi, P., Helfi, R., Modarres, R., Esfahani, P. M. & Dehno, M. G. 2020 A new approach to explore climate change impact on rainfall intensity–duration–frequency curves. *Theor. Appl. Climatol.* **142** (3), 911–928.

Soudi, M., Ahmadi, H., Yasi, M. & Hamidi, S. A. 2017 Sustainable restoration of the Urmia Lake: history, threats, opportunities and challenges. *Europ. Water* **60**, 341–347.

Tabari, H. & Talaee, P. H. 2011 Temporal variability of precipitation over Iran: 1966–2005. *J. Hydrol.* **396**, 313–320.

Taheri, M., Emadzadeh, M., Gholizadeh, M., Tajrishi, M., Ahmadi, M. & Moradi, M. 2019 Investigating the temporal and spatial variations of water consumption in Urmia Lake River Basin considering the climate and anthropogenic effects on the agriculture in the basin. *Agric. Water Manage.* **213**, 782–791.

Taylor, K. E., Stouffer, R. J. & Meehl, G. A. 2012 An overview of CMIP5 and the experiment design. *B Am. Meteorol. Soc.* **93**, 485–498.

Tourian, M. J., Elmi, O., Chen, Q., Devaraju, B., Roohi, S. h. & Sneeuw, N. 2015 A spaceborne multisensor approach to monitor the desiccation of Lake Urmia in Iran. *Remote. Sens. Environ.* **156**, 349–360.

Van Vuuren, D. P., Edmonds, J., Kainuma, M., Riahi, K., Thomson, A., Hibbard, K., Hurtt, G. C., Kram, T., Krey, V., Lamarque, J.-F., Masui, T., Meinshausen, M., Nakicenovic, N., Smith, S. J. & Rose, S. K. 2011 The representative concentration pathways: an overview. *Clim. Change* **109**, 5.

Wang, X., Hou, X. & Zhao, Y. 2021 Changes in consecutive dry/wet days and their relationships with local and remote climate drivers in the coastal area of China. *Atmos. Res.* **247**, 105138.

Wilks, D. S. 2011 *Statistical Methods in the Atmospheric Sciences*, 3rd edn. Academic Press. Oxford.

Xu, Y., Gao, X., Giorgi, F., Zhou, B., Shi, Y., Wu, J. & Zhang, Y. 2018 Projected changes in temperature and precipitation extremes over China as measured by 50-yr return values and periods based on a CMIP5 ensemble. *Adv. Atmos. Sci.* **35**, 376–388.

Zamani Nuri, A., Farzaneh, M. & Espanayi, K. 2014 Assessment of climatic parameters uncertainty under effect of different downscaling techniques. *Int. Res. J. Appl. Basic Sci.* **8**, 838–225.

Zarrin, A. & Dadashi-Roudbari, A. 2021 Projection of future extreme precipitation in Iran based on CMIP6 multi-model ensemble. *Theor. Appl. Climatol.* **144** (1), 643–660.

Zarrin, A., Dadashi-Roudbari, A. & Hassani, S. 2022 Future changes in precipitation extremes over Iran: insight from a CMIP6 bias-corrected multi-model ensemble. *Pure Appl. Geophys.* **179**, 441–464.

Zhang, X. & Yang, F. 2004 *RClimDex (1.0) User Manual*. Climate Research Branch Environment Canada, Downsview, Ontario. https://acmad.net/rcc/procedure/RClimDexUserManual.pdf.

First received 3 November 2022; accepted in revised form 27 June 2023. Available online 12 July 2023